Dust-acoustic periodic travelling waves in a magnetized dusty plasma with trapped ions and nonthermal electrons in astrophysical situations:Oblique excitations

E. F. El-Shamy
King Khalid University
M. M. Selim (mselim2000@yahoo.com)
Damietta University

Research Article

Keywords: Dusty plasma, Schamel equation, bifurcation theory, dust-acoustic periodic traveling waves. trapped ions, nonthermal fast electrons

Posted Date: August 1st, 2022

DOI: https://doi.org/10.21203/rs.3.rs-1893704/v1

Dust-acoustic periodic travelling waves in a magnetized dusty plasma with trapped ions and nonthermal electrons in astrophysical situations:Oblique excitations

E. F. El-Shamy[1,2].M. M. Selim[2]

[1] Department of Physics, College of Science, King Khalid University, P. O. 9004, Abha, Saudi Arabia

[2] Department of Physics, Faculty of Science, Damietta University, New Damietta City, P. O. 34517, Egypt

Abstract Obliquely propagating three-dimensional dust-acoustic periodic travelling waves (DAPTWs) has been undertakenin a magnetized dusty plasma composed of negatively charged inertial dust particles, trapped ions, and nonthermal fast electrons. In a dusty plasma model at hand, the dynamic behaviors of DAPTWs are governed by a Schamel equation. The presence of dust acoustic solitary waves (DASWs) and DAPTWs is investigated via bifurcation analysis of the Hamiltonian system. In the nonlinear regime, the Sagdeev potential and phase portrait structures indicate the presence of small-amplitude DAPTW solutions. The influences of intrinsic physical parameters include the strength of the static magnetic field, the obliqueness of propagation,the thermal pressure of charged dust grains, the electron to dust density ratio, the trapping parameter of trapped ions and the degree of nonthermality of fast electrons on the characteristics of DAPTWs are simulated numerically. In particular, the findings illustrate that the amplitude of DAPTWs is reduced as the numerical values of the trapping parameterare decreased. Interestingly, the numerical results of the theoretical simulations can be used to significantly highlight the physical nature of DAPTWs in astrophysical situations such as Earth's magnetosphere, auroral region, and heliospheric environments.

Keywords

Dusty plasma, Schamel equation, bifurcation theory, dust-acoustic periodic traveling waves. trapped ions, nonthermal fast electrons.

* CorrespondenceE-mail: mselim2000@yahoo. com

1. Introduction

The trapping of electrons and ions in a dusty plasma is an interesting nonlinear phenomenon. In this situation, the electrostatic wave potential confines some charged particles (i.e., electrons and ions) in a certain region in the dusty plasma model, and these particles are forced to bounce back and forth. In dusty plasma system, the inertia is well known to be provided by the mass of dust grains, whereas the restoring force comes from the pressures of inertialess ions and electrons (Mamun et al. 1996). Negative charged dusty plasmas are usually dominated due to the flow of plasma currents to their surfaces. Hence, the trapping process makes the electron and ion species deviate from Maxwellian distribution; therefore, they follow non-thermal distribution functions depending on the laboratory and space plasma environment under consideration. One of the most commonly non-thermal distribution functions which describe the trapping process of the electron and ion species in many laboratory and space plasmas is the Schamel distribution function (Schamel 1972, 1973, 1986). In general, many investigators have studied the effects of trapped ions on the nonlinear waves for different plasma models (Mamun 1998; Adhikary et al. 2014, 2017; Dev et al. 2015a, 2015b; El-Hanbaly et al. 2015; Misra and Wang 2015; Sultana 2921). For example, a theoretical investigation of dust acoustic solitary waves (DASWs) in an unmagnetized three component dusty plasma consists of negative dust fluid, free electrons, trapped and free ions is studied by (Mamun1998). Due to the departure of trapped ions from the Boltzmann distribution, the small amplitude dust acoustic waves (DAWs) dynamics are governed by a Korteweg-de-Vries (KdV) type equation. Moreover, several authors have shown that the trapped ion species substantially affect the profile of dust acoustic shock waves (Adhikary et al. 2014, 2017; Dev et al. 2015a, 2015b; El-Hanbaly et al. 2015). In addition, many space and laboratory observations indicate the existence of electrons with high energies that do not obey Boltzmann distribution. Instead, the distribution of electron energy, frequently has more complicated shapes with long tails, modeled by a nonthermal distribution (Cairns et al. 1995; Saha and Chatterjee 2009; Mamun and Shukla 2009; Selim 2016). The first attempt which describes the energetic electrons observed by FREJA satellite using the nonthermal

distribution was developed by Cairns et al. 1995. Later, the existence of nonthermal electrons in various astrophysical environments, such as solar wind, magnetosphere, interstellar medium, and auroral zone plasmas (Cairns et al. 1995; Saha and Chatterjee 2009; Mamun and Shukla 2009; Selim 2016; Lundin et al. 1989; Futaana et al. 2003; Gill et al. 2007), was confirmed by the Vela satellite (Lundin et al. 1989). Also, the disappearance of energetic electrons from the upper ionosphere of Mars has been recorded by the ASPERA on the Phobos 2 satellite. The effects of electrons nonthermal distribution and the polarity of dust charge number density on nonplanar spherical and cylindrical DIASWs are investigated by Mamun and Shukla (2009) and Selim (2016). It is observed that the features of the DIASWs are significantly modified by the effects of the nonthermality of the electrons distribution and the geometry factor (Mamun and Shukla 2009). Misra and Wang (2015) have investigated the nonlinear characteristics of DAWs in magnetized dusty plasma, including negative charge dust fluid, vortex-like ions distribution, and nonthermal fast electrons. They demonstrated that under a critical value of the percentage of energetic electrons, the excitation of DAWsvanishes.

In recent years, the bifurcation theory (Show and Hale 1980) has become one of the most interesting and famous approaches to study the dynamical behaviour of plasma systems. In this sense, the bifurcation analysis of the phase portrait for the Hamiltonian of the system has been extensively employed to study the physical nature of travelling nonlinear dust acoustic waves in plasma. This analysis has significant applications in different plasma environments (Selim et al.2015; Abdelwahed et al. 2017; El-Shamy et al.2021; Abdikian 2021; Selim et al.2021; Samanta et al.2013; Pradhan et al. 2021; Tolba 2021). For instance, Selim et al. (2015) have investigated the bifurcation analysis of nonlinear ionacoustic travelling waves in a multicomponent magnetoplasma with superthermal electrons. The propagation of nonlinear dust ion acoustic periodic waves (DIAPWs) in a dusty plasma consists of stationary charged dust grains, cold ions, and two temperature superthermal electrons is studied by Abdelwahed et al. (2017). Recently, the bifurcation method has been employed to study the nonlinear and supernonlinear ion acoustic waves in electron-ion plasmas with electrons obey generalized (r, q)-distribution

by Abdikian (2021). Also, El-Shamy et al. (2020) applied the bifurcation approach to study the properties of the nonlinear acoustic waves in a magnetized ultrarelativistic degenerate plasma composed of warm fluid ions ultrarelativistic degenerate inertialess electrons and positrons and immobile heavy negative ions. Then, Selim et al. (2021) studied the effects of trapped ions concentration on the dust acoustic solitary and periodic travelling waves dynamics in a dusty plasma consisting of dust fluid, trapped ions, and Maxwellian electrons.

However, in the light of the previous discussion, the influences of the trapped ions, nonthermal electrons, the strength of the external static magnetic field, and the obliqueness of propagation on the physical behaviour of DAPTWs in dusty plasma seem to be a vital problem; thus, it will be the target of this work. This paper is organized as follows: the mathematical model for a magnetized dusty plasma composed of negatively charged inertial dust particles, trapped ions, and nonthermal fast electrons is presented in section 2. Furthermore, Schamel equation (i. e., Korteweg-de-Vries(KdV) type equation) that governs the dynamics of nonlinear waves propagating in the current plasma is derived. Sagdeev potential and bifurcation analysis are developed to examine the possibility DAPTWs existence in section 3. Finally, numerical simulations, results, and discussions are outlined in section 4.

2. Model equations

In the present work, we consider a magnetized three-component plasma system consists of collisionless, massive, micrometer-sized, dust grains with negative charge, ions with trapped particles and nonthermally distributed fast electrons. An external magnetic field is applied in the z-direction (i. e. $\mathrm{B} = \mathrm{B}_0\hat{\mathrm{z}}$). The propagation of low frequency, compared to the dust cyclotron frequency, DAWs in this system is governed by the following set of normalized coupled nonlinear partial differential equations (Shukla and Mamun 2002; Fortov et al. 2005):

$$\frac{\partial \mathrm{N_d}}{\partial \tau} + \frac{\partial}{\partial \mathrm{X}}(\mathrm{N_d U_{dx}}) + \frac{\partial}{\partial \mathrm{Y}}(\mathrm{N_d U_{dy}}) + \frac{\partial}{\partial \mathrm{Z}}(\mathrm{N_d U_{dz}}) = 0, \tag{1}$$

$$\frac{\partial \mathrm{U_{dx}}}{\partial \tau}+\mathrm{U_{dx}}\frac{\partial \mathrm{U_{dx}}}{\partial \mathrm{X}}+\mathrm{U_{dy}}\frac{\partial \mathrm{U_{dx}}}{\partial \mathrm{Y}}+\mathrm{U_{dz}}\frac{\partial \mathrm{U_{dx}}}{\partial \mathrm{Z}}=\frac{\partial \Phi}{\partial \mathrm{X}}-\frac{5}{3}\sigma \mathrm{N_d^{-1/3}}\frac{\partial \mathrm{N_d}}{\partial \mathrm{X}}+\omega_c \mathrm{U_{dy}}, \quad (2)$$

$$\frac{\partial \mathrm{U_{dy}}}{\partial \tau}+\mathrm{U_{dx}}\frac{\partial \mathrm{U_{dy}}}{\partial \mathrm{X}}+\mathrm{U_{dy}}\frac{\partial \mathrm{U_{dy}}}{\partial \mathrm{Y}}+\mathrm{U_{dz}}\frac{\partial \mathrm{U_{dy}}}{\partial \mathrm{Z}}=\frac{\partial \Phi}{\partial \mathrm{Y}}-\frac{5}{3}\sigma \mathrm{N_d^{-1/3}}\frac{\partial \mathrm{N_d}}{\partial \mathrm{Y}}-\omega_c \mathrm{U_{dx}}, \quad (3)$$

$$\frac{\partial \mathrm{U_{dz}}}{\partial \tau}+\mathrm{U_{dx}}\frac{\partial \mathrm{U_{dz}}}{\partial \mathrm{X}}+\mathrm{U_{dy}}\frac{\partial \mathrm{U_{dz}}}{\partial \mathrm{Y}}+\mathrm{U_{dz}}\frac{\partial \mathrm{U_{dz}}}{\partial \mathrm{Z}}=\frac{\partial \Phi}{\partial \mathrm{Z}}-\frac{5}{3}\sigma \mathrm{N_d^{-1/3}}\frac{\partial \mathrm{N_d}}{\partial \mathrm{Z}}, \quad (4)$$

$$\frac{\partial^2 \Phi}{\partial \mathrm{X}^2}=\mathrm{N_d}+\delta \mathrm{N_e}-\mu \mathrm{N_i}. \quad (5)$$

In Eqs. (1)-(5) X, Y, Z and τ are the space coordinates and time, normalized by the Debye length $\lambda_D = (K_B T_i/4\pi e^2 Z_d n_{do})^{1/2}$ and the dust plasma period $\omega_{pd}^{-1} = (m_d/4\pi Z_d n_{do} e^2)^{1/2}$, respectively. The electron, ion and dust number densities, N_e, N_i and N_d are normalized by the unperturbed dust number density, N_{d0}. Also, U_{dx}, U_{dy}, U_{dz} are the dust fluid speed in X, Y, Z directions and Φ is the electrostatic potential which are normalized by the dust acoustic speed, $C_d = (Z_d K_B T_i/m_d)^{1/2}$, and $K_B T_i/e$, respectively, with K_B denotes the Boltzmann constant and T_i is the ion thermal temperature. The ratios, $\delta = \frac{N_{e0}}{Z_d N_{d0}}$ and $\mu = \frac{N_{i0}}{Z_d N_{d0}}$ are the number density ratios which satisfy the neutrality condition of charge, $\mu = \delta + 1$, at the equilibrium state. The temperature ratio, $\sigma = T_d/T_i$, is dust to ion thermal temperature ratio and $\omega_c = \frac{|Z_d|B_0}{m_d \omega_{pd}}$ is the dust-cyclotron frequency normalized by the dust plasma oscillation frequency, ω_{pd}. Since the thermal motion of charged dusts cannot keep up with the dust acoustic wave propagation, we have considered an adiabatic compression of the dust fluid, and use the pressure law

$$P_d = N_{d0} K_B T_d \left(\frac{N_d}{N_{d0}}\right)^{\gamma}. \quad (6)$$

In Eqs. (1)-(3), where $\gamma = (N+2)/N$, and N is the number of degrees of freedom. In the present work $N = 3$, for three-dimensional configuration and hence, $\gamma = 5/3$.

It is assumed that the DAWs, propagating in this system, has low phase velocity, $\lambda (= \omega/k)$, compared to the thermal velocities of ions and electrons, i. e. ($v_{td} << \lambda << v_{ti}, v_{te}$) (Mamun 1998). Hence, $v_{tJ} = \sqrt{k_B T_J/m_J}$, where m_J and $T_J, J = d, i, e$, being the

mass and thermal temperature of dust, ions and electrons, respectively. In the current model the electron temperature is much greater than ion temperature (i. e. $T_e >> T_i$) and $n_{i0} >> n_{e0}$. It is assumed that the thermal conductivity, the effects of viscosity and the energy transfer due to collisions are negligible. In addition, the magnetic pressure is considered to be larger than thermal plasma pressure and the dust grains charging is constant. Since we are dealing with ions with trapped particles distribution functions (Cairns et al. 1995; Mamun 1998; Misra and Wang 2015) the ion number density,n_i, is given in terms of the electrostatic potential, Φ, at the small amplitude limit, as (Mamun 1998)

$$n_i \simeq 1 - \Phi - \frac{4}{3}\frac{(1-\beta)}{\sqrt{\pi}}(-\Phi)^{3/2} + \frac{1}{2}\Phi^2, \tag{7}$$

where the term $-\frac{4}{3}\frac{(1-\beta)}{\sqrt{\pi}}(-\Phi)^{3/2}$ in the expansion of n_i represents the contribution of trapped ions. The case $\beta = 0$, represents the plateau or flat-topped distribution and $\beta = 1$ corresponds to the Boltzmann distribution of ions. On the other side, the electrons are assumed to obey non-thermal distribution. Thus, the electron number density, n_e, can be expanded as

$$n_e = (1 - \alpha\vartheta\Phi + \alpha\vartheta^2\Phi^2)\, exp(\vartheta\Phi), \tag{8}$$

where $\vartheta = \frac{T_i}{T_e}$, is electron to ion thermal temperature ratio. The nonthermality parameter is $\alpha = \frac{4a}{1+3a}$ with $a > 0$, represents the degree of nonthermality of the charged particles or the percentage of energetic or fast electrons in the plasma, and $\alpha < 1$ (> 1) corresponds to $a < 1$ (> 1). The value $a = 0$ corresponds to the case of thermal equilibrium (Boltzmann distribution) of electrons.

To derive the nonlinear KdV type equation for the small amplitude DAWs from Eqs. (1) to (5), we have to find an appropriate coordinate frame where the wave can be described smoothly. For this purpose, the reductive perturbation technique (RPT) (Washimi and Tanuiti 1966) is applied as powerful tool to derive the KdV type equation for the propagation of DA waves in the plasma system. According to the RPT, the independent variables in Eqs. (1) to (5), are stretched as

$$\zeta = \varepsilon^{1/4}(L_x X + L_y Y + L_z Z - \lambda T) = \varepsilon^{1/4}(\eta - \lambda T), T = \varepsilon^{3/4}\tau, \quad (9)$$

where ε is a small parameter, measures the weakness of the wave amplitude, and λ is the wave phase velocity normalized by the dust acoustic velocity, C_d. The direction cosines, L_x, L_y and L_z of the wave vector along the axes, X, Y and Z satisfy the equality; $L_x^2 + L_y^2 + L_z^2 = 1$. The dependent variables $N_d, U_{dx,y,z}$and Φ, in Eqs. (1) to (8), can be expanded as

$$N_d = 1 + \varepsilon N_d^{(1)} + \varepsilon^{3/2} N_d^{(2)} + \varepsilon^2 N_d^{(3)} + \cdots, \quad (10)$$

$$U_{dx} = \varepsilon^{5/4} U_{dx}^{(1)} + \varepsilon^{3/2} U_{dx}^{(2)} + \varepsilon^2 U_{dx}^{(3)} + \cdots, \quad (11)$$

$$U_{dy} = \varepsilon^{5/4} U_{dy}^{(1)} + \varepsilon^{3/2} U_{dy}^{(2)} + \varepsilon^2 U_{dy}^{(3)} + \cdots, \quad (12)$$

$$U_{dz} = \varepsilon U_{dz}^{(1)} + \varepsilon^{3/2} U_{dz}^{(2)} + \varepsilon^2 U_{dz}^{(3)} + \cdots, \quad (13)$$

$$\Phi = \varepsilon \Phi^{(1)} + \varepsilon^{3/2} \Phi^{(2)} + \varepsilon^2 \Phi^{(3)} + \cdots. \quad (14)$$

Now, substituting these expansions into Eqs. (1) to (5),and collecting the terms of different powers of ε, in the lowest order, we obtain

$$\frac{\partial N_d^{(1)}}{\partial \eta} = \frac{L_z}{\lambda} \frac{\partial U_{dz}^{(1)}}{\partial \eta}, \quad (15) \qquad \frac{\partial U_{dz}^{(1)}}{\partial \eta} = \frac{5}{3} \frac{\sigma L_z}{\lambda} \frac{\partial N_d^{(1)}}{\partial \eta} - \frac{L_z}{\lambda} \frac{\partial \Phi^{(1)}}{\partial \eta}, \quad (16)$$

$$N_d^{(1)} = -[\mu + \delta\vartheta(1-\alpha)]\Phi^{(1)}. \quad (17)$$

From these equations one can derive the phase velocity as

$$\lambda = L_z \sqrt{\left[\frac{1}{(\mu + \delta\vartheta(1-\alpha))} + \frac{5}{3}\sigma\right]}. \quad (18)$$

Equation (18) represents the phase velocity of the DAWs propagate with the velocity, λ,which must be real valued. For λ to be real the expression in the square brackets of Eq. (18) must be positive,which gives $\alpha > \alpha_c = 1 + \frac{1}{\delta\vartheta}\left(\mu + \frac{5}{3}\right)$. This means that DAWs propagate in the current plasma system when the percentage of nonthermalenergetic electrons exceeds some critical value. For the next order of ε, we obtain

$$\frac{\partial N_d^{(2)}}{\partial \eta} = \frac{1}{\lambda}\frac{\partial N_d^{(1)}}{\partial T} + \frac{L_x}{\lambda}\frac{\partial U_{dx}^{(2)}}{\partial \eta} + \frac{L_y}{\lambda}\frac{\partial U_{dy}^{(2)}}{\partial \eta} + \frac{L_z}{\lambda}\frac{\partial U_{dz}^{(2)}}{\partial \eta}, \tag{19}$$

$$\frac{\partial U_{dz}^{(2)}}{\partial \eta} = \frac{1}{\lambda}\frac{\partial U_{dz}^{(1)}}{\partial T} - \frac{L_z}{\lambda}\frac{\partial \Phi^{(2)}}{\partial \eta} + \frac{5}{3}\sigma L_z \frac{\partial N_d^{(2)}}{\partial \eta}, \tag{20}$$

$$N_d^{(2)} = \frac{\partial^2 \Phi^{(2)}}{\partial \eta^2} - \frac{4}{3}\frac{\mu(1-\beta)}{\sqrt{\pi}}(-\Phi^{(1)})^{3/2} - c\Phi^{(2)}, \tag{21}$$

$$U_{dx}^{(2)} = -\frac{\lambda L_x}{\omega_c^2}\left(1 + \frac{5}{3}\sigma(\mu + \delta\vartheta(1-\alpha))\right)\frac{\partial^2 \Phi^{(1)}}{\partial \eta^2}, \tag{22}$$

$$U_{dy}^{(2)} = -\frac{\lambda L_y}{\omega_c^2}\left(1 + \frac{5}{3}\sigma\big(\mu + \delta\vartheta(1-\alpha)\big)\right)\frac{\partial^2 \Phi^{(1)}}{\partial \eta^2}. \tag{23}$$

Now, by eliminating the second-order perturbed terms and their derivatives from Eqs. (19) - (23) and substituting the first-order perturbed quantities from Eqs. (15) -(17), we obtain the following Schamel (KdV type) equation:

$$\frac{\partial \Phi^{(1)}}{\partial \tau} + A\sqrt{-\Phi^{(1)}}\frac{\partial \Phi^{(1)}}{\partial \zeta} + B\frac{\partial^3 \Phi^{(1)}}{\partial \zeta^3} = 0, \tag{24}$$

where

$$A = \frac{1-\beta}{\sqrt{\pi}\lambda}\frac{\mu L_z^2}{(\mu + \delta\vartheta(1-\alpha))^2}, \tag{25}$$

$$B = \frac{\lambda\big(3 + (\mu + \delta\vartheta(1-\alpha))\big)(5\sigma - 3\lambda^2)}{6\omega_c^2(\mu + \delta\vartheta(1-\alpha))} + \frac{L_z^2}{2\lambda(\mu + \delta\vartheta(1-\alpha))^2}. \tag{26}$$

3- DASW and DAPTW bifurcation points

We now apply the bifurcation theory (Shaw and Hale 1980; Selim et al.2015; Abdelwahed et al. 2017; El-Shamy et al.2021; Abdikian 2021; Selim et al.2021; Samanta et al.2013; Pradhan et al. 2021; Tolba 2021) to study the presence of DASW and DAPTWsolutions of Eq. (24). Our starting point here is the analysis of Tolba (2021) that establishes the existence of DASW and DAPTW for a Schamel equation. We assume that the DASWs and DAPTWs move with a constant wave speed $\nu > 0$ and introduce the change of coordinates $\xi = \zeta - \nu\tau$. Accordingly, Schamel Eq. (24) can be transformed,

using $\Phi^{(1)}(\zeta,\tau)=\Phi(\xi)$, into

$$\frac{d^2\Phi}{d\xi^2}=\frac{\nu}{B}\Phi+\frac{2A}{3B}(-\Phi)^{3/2}. \tag{27}$$

The Hamiltonian system for Eq.(27) can be obtained by setting $\frac{d\Phi}{d\xi}=\varphi$, resulting in first-order differential equations that can be written as:

$$\begin{aligned}\frac{d\Phi}{d\xi}&=\varphi,\\ \frac{d\varphi}{d\xi}&=\frac{\nu}{B}\Phi+\frac{2A}{3B}(-\Phi)^{3/2}.\end{aligned} \tag{28}$$

We are interested in finding the DASW and DAPTW solutions to the Hamiltonian system (28), numerically. Therefore, one can express the Hamiltonian system in terms of Hamiltonian function $H(\Phi,\varphi)$ as follows:

$$H(\Phi,\varphi)=\frac{\varphi^2}{2}+\frac{4A}{15B}(-\Phi)^{5/2}-\frac{\nu}{2B}\Phi^2=h, \tag{29}$$

Where h is the constant thatdetermines the value of the energy. In addition, one can adapt Eq. (27) to express the potential, V(Φ), that is

$$V(\Phi)=\frac{4A}{15B}(-\Phi)^{5/2}-\frac{\nu}{2B}\Phi^2. \tag{30}$$

The Hamiltonian system (28) admits the following two equilibrium points on the axis $\varphi=0$ and $F(\Phi)\left(=\frac{\nu}{B}\Phi+\frac{2A}{3B}(-\Phi)^{3/2}=0\right)$: $E_i(\Phi_i,0)$, where $\Phi_0=0,\Phi_1=-\left(\frac{3\nu}{2A}\right)^2$ and $i=0$ and 1, respectively. Furthermore, the determinant of the Jacobi matrix corresponding to Eq. (28) admits the following expression

$$\det|J(\Phi_i,0)|=\left|\begin{pmatrix}0 & 1\\ \frac{\nu}{B}-\frac{A}{B}(-\Phi_i)^{1/2} & 0\end{pmatrix}\right|=-\frac{\nu}{B}+\frac{A}{B}(-\Phi_i)^{1/2}. \tag{31}$$

Based on the mathematical analysis of the planar dynamic system, the equilibrium points$E_i(\Phi_i,0)$ of the Hamiltonian system (28) is either saddle pointif $\det|J(\Phi_i,0)|<0$or center point if $\det|J(\Phi_i,0)|>0$ or cusp point if $\det|J(\Phi_i,0)|=0$. Now let us determine energy values, h, at the equilibrium points $E_i(\Phi_i,0)$. Then, at the equilibrium point $E_0(0,0)$, the energy value $h=H(0,0)\cong 0$. Moreover, the energy value $h=$

$H\left(-\left(\frac{3v}{2A}\right)^2, 0\right) \cong -\frac{v^5}{2BA^4}$ at the equilibrium point $E_1\left(-\left(\frac{3v}{2A}\right)^2, 0\right)$. We now identify different curves in the phase portraits depending on the equilibrium points $E_i(\Phi_i, 0)$. As displayed in Fig. 1, the saddle point of the solid curve is at $h \cong 0$, where $det|J(0,0)| = -\frac{v}{B} < 0$, ensures DASW solutions. These types of curves are called nonlinear homoclinic trajectories. In addition, the center point of the close dashed curve with no separatrixis at $h < 0$, where $det|J(0,0)| = \frac{v}{2B} > 0$, guarantees DAPTW solutions. These types of closed curves are named nonlinear heteroclinic cycles. This paper will focus on the center point of DAPTW solutions.

Fig.1. Phase portrait of the dynamical system (28) for $L_z = 0.1, \delta = 1.5, \sigma = 0.10, \beta = -2.5, \alpha = 0.01$ and $\omega_c = 0.05$.

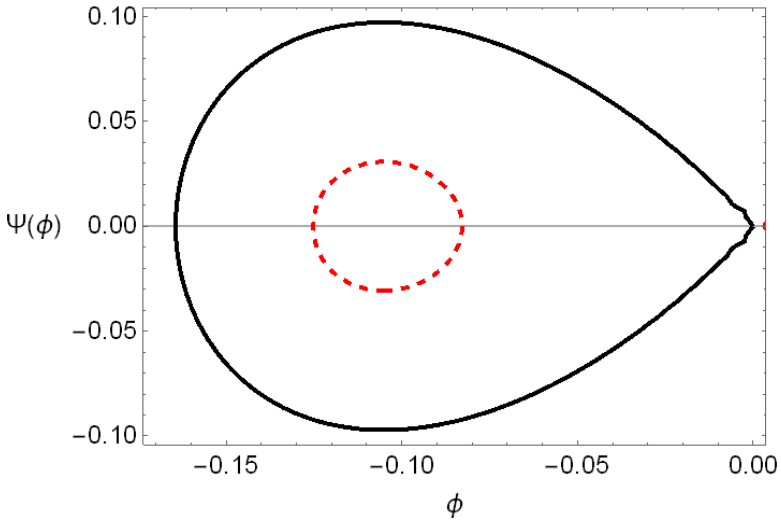

4. Numerical investigations

In this part, we will test the DASW and DAPTW bifurcation points by numerical simulations to verify the predictions given by bifurcation analysis. Accordingly, we have carried the numerical simulations over a wide range of plasma parameters. In this study, the numerical values of the applied parameters were frequently used in many literature (Mamun 1998; Misra and Wang 2015), for example, in space plasmas (such as Earth's magnetosphere, auroral region, heliospheric environments) and laboratory dusty plasma

situations. For this purpose, we choose some of the normalized physical parameters in plasma, such as (Mamun 1998; Misra and Wang 2015) $L_z \approx 0.1-0.2, \delta \approx 0.4-2.5, \sigma \approx 0.10-0.12, \beta \approx -1.5—-3, \alpha \approx 0.01-1.5$ and $\omega_c \approx 0.3-0.5$. It should be mentioned here that we complemented the work done in (Mamun 1998; Misra and Wang 2015), which concentrated on the behavior of DASWs. Whereas, in this work, we will focus on the physical nature and numerical simulation of the Sagdeev potential,$V(\Phi)$,and DAPTWs. So, we did not include DASWs figures here. Now we present the numerical representation of Eq.(30) (i. e., the Sagdeev potential,$V(\Phi)$) by changing the values of the obliqueness of wave propagation, L_z, the ratio of unperturbed electron density to the unperturbed dust density, δ, the ratio of dust to electron temperature, σ, free ion-trapped ion temperature ratio, β, the nonthermal parameter, α, the dust-cyclotron frequency, ω_c. As shown in Figs. 2-7, the negative deep values of $V(\Phi)$ are dependent on $L_z, \delta, \sigma, \beta, \alpha,$ and ω_c. Obviously, there are two values given for Φ(i. e.,$\Phi_0 = 0$and $\Phi_1 = -(3v/2A)^2$)), where $V(\Phi)$ becomes zero. Clearly,$V(\Phi)$is defined physically as a pseudoparticle that periodically oscillates back and forth in the potential well between two zeroes points. Figure 2 illustrates that both depth and amplitude of $V(\Phi)$ increase with the decrease in the obliqueness of propagation, L_z.Furthermore, increasing $\delta(\sigma)$leads to an increase (slightly increase) of the $V(\Phi)$depth and amplitude, as shown in Fig. 3(4), respectively. For $\beta < 0$ (i. e.,a vortex-like excavated trapped ion distribution), Fig.5 demonstrates that the depth and amplitude of V(Φ) decrease with the decrease in the numerical values of β. Figure 6 shows that $V(\Phi)$ depth and amplitude are slightly enhanced with decreasing α. As shown in Fig.7, an increase in the dust-cyclotron frequency, ω_c, leads to an increase in $V(\Phi)$depth, but the amplitude would remain constant. It is interesting to note that enhancing the depth of $V(\Phi)$makes DAPTWs narrower. Therefore, we can expect physically, as will be discussed in the following paragraphs, that the growth in δ, σ, β and ω_c makes DAPTWs more spiky, but a rise in L_z and α makes the DAPTWs broader and shorter.

To complete the picture, we must also include the influences of the plasma parameters; $L_z, \delta, \sigma, \beta, \alpha$ and ω_c on the structures of DAPTWsolutions. First of all, we can numerically find the DAPTW solutions via Mathematica software. Figures 8-13 show the profiles of the DAPTWs as a function in the space coordinate,ξ, at various values of $L_z, \delta, \sigma, \beta, \alpha$ and ω_c, respectively. Figure 8 shows that the DAPTWs become less deep (amplitude) and wider as L_z increases. Figure 9 (10) displays that the amplitude and the width of DAPTWs increase (increase slightly) with an increase in $\delta(\sigma)$. For $\beta < 0$, Fig.11 demonstrates that DAPTWs become more profound and broader with an increase in the numerical valuesof β. The amplitude of DAPTWs increases slightly with decreasing α, as displayed in Fig. 12. Also, increasing ω_c leads to a reduction in the width of DAPTWs, while the amplitudeof DAPTWswillremain fixed, as shown in Fig.13.

From a physical point of view, decreasing L_z (i. e., increasing θ, where θ is the angle that the propagation vector of DAPTWs makes with the magnetic field), leads to a growth (a reduction) in the amplitude (width) of DAPTWs. Therefore, one can expect that as the DAPTWs approach the direction normal to the magnetic field (i. e.,$L_z \rightarrow 0$), the amplitudes of DAPTWs increase to maximum value, and the width decrease tominimum value. A reduction in the electron concentration gives an increase in the dust concentration to keep the quasineutrality in the dusty plasma model (where $\delta = n_e^{(0)}/Z_d n_d^{(0)}$, and $n_i^{(0)} = n_e^{(0)} + Z_d n_d^{(0)}$). Thus, the driving force provided by dust inertia in DAPTWs increases; hence, the amplitude of DAPTWs is enhanced. The slight growth in the amplitude is a result of the rise in the fraction of thermal dust grains, σ, which is one of the sources of energy for DAPTWs. Growth in the numerical values of β gives a decrease in the nonlinear coefficient, A, that causes an increase in the amplitude, which means an increase in the energy of the DAPTWs. An increase in the degree of nonthermality of electrons, α (i. e.,the percentage of fast electrons in the plasma) leads to a decrease in the phase velocity, λ, which, in turn, leads to an enhancement of the nonlinear coefficient leading to a reduction in the amplitude of DAPTWs. Interestingly, the degree of nonthermality of electrons has a weak effect on the physical nature of DAPTWs. An increase in the

numerical values of the external uniform magnetic field, B_0, increases the ion cyclotron frequency, ω_c, and decreasesthe dispersion of model plasma at hand. Thus, the static constant magnetic field constrains the charged particles of plasma; a condition referred to as magnetic confinement. Therefore, the uniform external magnetic field makes DAPTWs structures more spiky.

To conclude, a plasma model of warm negative dust fluid including trapped positive ions and nonthermal fast electrons has been examined. The physical nature of the small but finite amplitude of DAPTWs has been addressed. The basic features of DAPTWs are changed due to the existence of nonthermal electrons and positive trapped ions. The plasma model at hand gives only rarefactive DAPTWs with features that depend strongly on the obliqueness of propagation, L_z, the ratio of unperturbed electron density to the unperturbed dust density, δ, free ion-trapped ion temperatureratio, β, the dust-cyclotron frequency, ω_c. Finally, we consider that our present discussion may help to understand the salient features of the DAPTWs in astrophysical environments such as Earth's magnetosphere, auroral region, and heliospheric environments.

Fig.2. (Colour online) The variation of the Sagdeev pseudopotential $V(\phi)$ versus ϕ, at different values of L_z for $\delta = 1.5, \sigma = 0.10, \beta = -2.5,$ $\alpha = 0.1$ and $\omega_c = 0.3$.

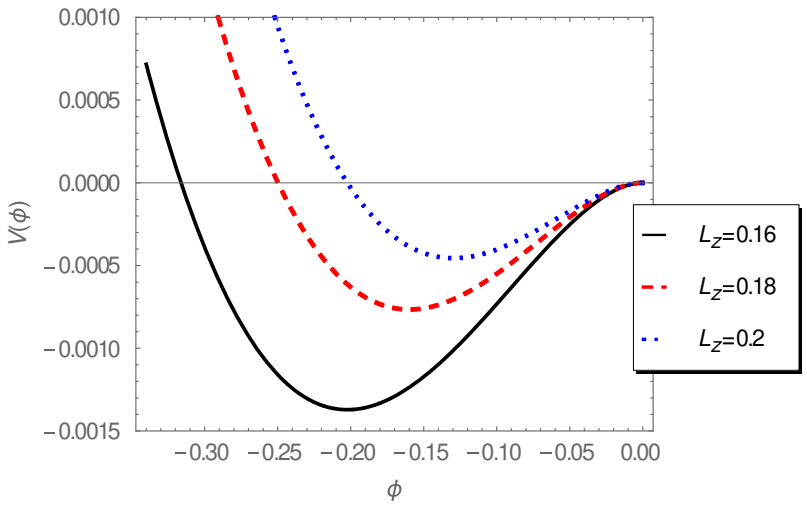

Fig.3. (Colour online) The variation of the Sagdeev pseudopotential $V(\phi)$ versus ϕ, at different values of δ for $L_z = 0.18, \sigma = 0.10, \beta = -2.5, \alpha = 0.1$ and $\omega_c = 0.3$.

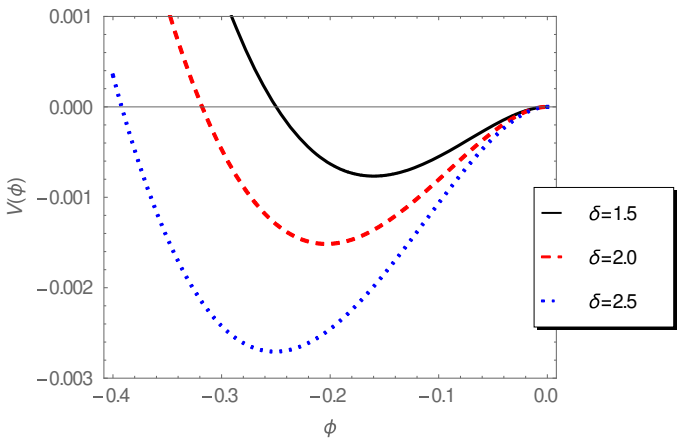

Fig.4. (Colour online) The variation of the Sagdeev pseudopotential $V(\phi)$ versus ϕ, at different values of σ for $L_z = 0.18, \delta = 1.5, \beta = -2.5, \alpha = 0.1$ and $\omega_c = 0.3$.

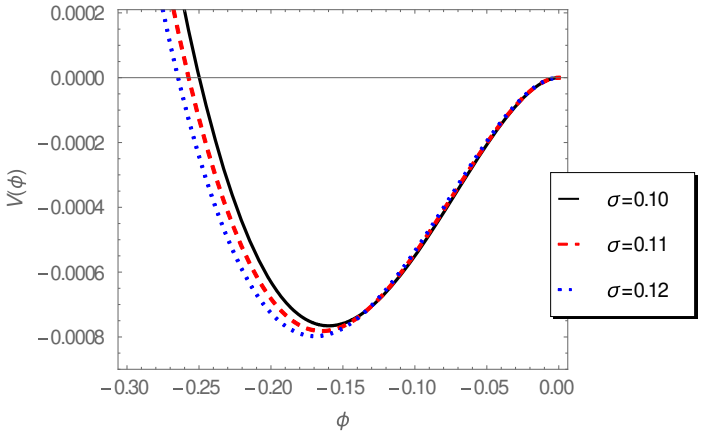

Fig.5. (Colour online) The variation of the Sagdeev pseudopotential $V(\phi)$ versus ϕ, at different values of$\sigma$for$L_z = 0.18, \delta = 1.5, \sigma = 0.1, \alpha = 0.1$ and $\omega_c = 0.3$.

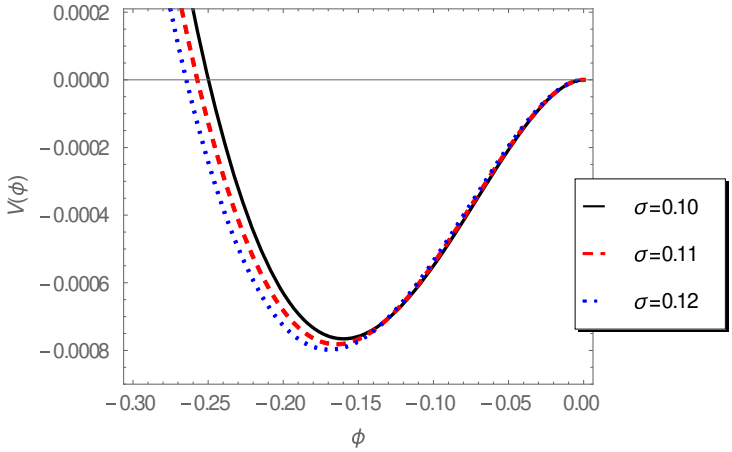

Fig.6. (Colour online) The variation of the Sagdeev pseudopotential $V(\phi)$ versus ϕ, at different values of α for $L_z = 0.18, \delta = 1.5, \sigma = 0.1, \beta = -2.5$ and $\omega_c = 0.3$.

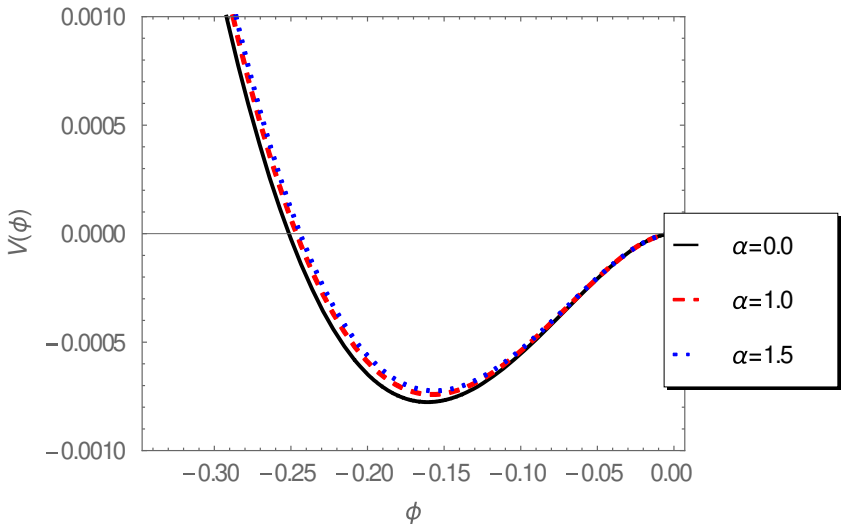

Fig.7. (Colour online) The variation of the Sagdeev pseudopotential $V(\phi)$ versus ϕ, at different values of ω_c for $L_z = 0.18, \delta = 1.5, \beta = -2.5$ and $\alpha = 0.1$.

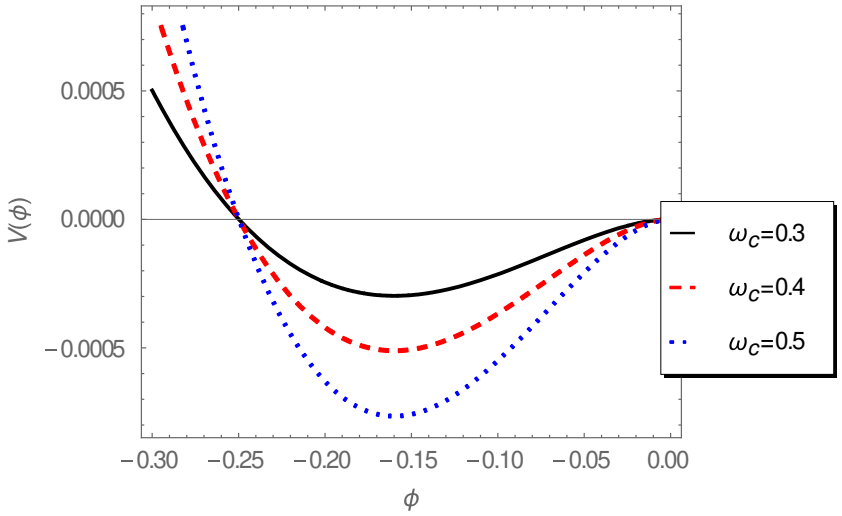

Fig.8. (Colour online) The evolution of the DAPTWs,ϕ, for different $L_z$for $\beta = -2.5, \delta = 1.5, \sigma = 0.1, \alpha = 0.1$ and $\omega_c = 0.3$.

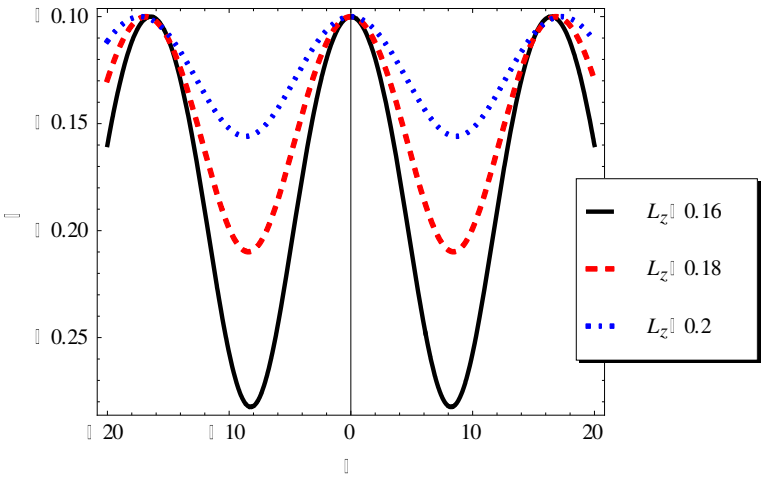

Fig.9. (Colour online) The evolution of the DAPTW,ϕ, for different values of δ at $L_z = 0.18$ for $\beta = -2.5, \sigma = 0.1, \alpha = 0.1$ and $\omega_c = 0.3$.

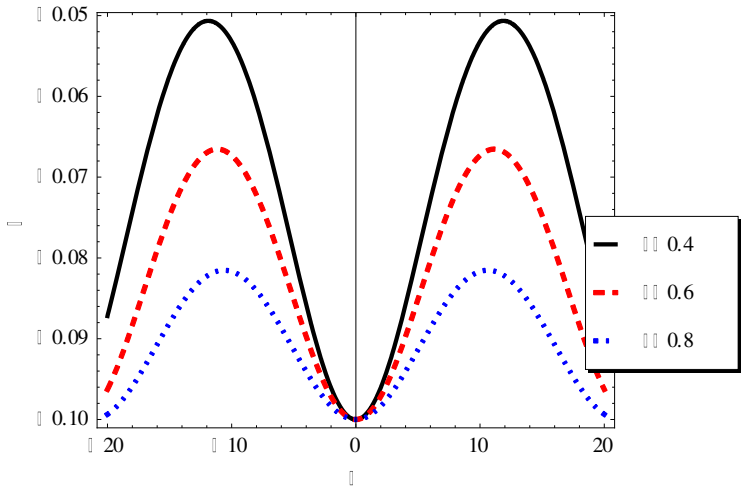

Fig.10. (Colour online) The evolution of the DAPTWs,ϕ, for different values of σ at $L_z = 0.18$, $\delta = 1.5, \beta = -2.5, \alpha = 0.1$ and $\omega_c = 0.3$.

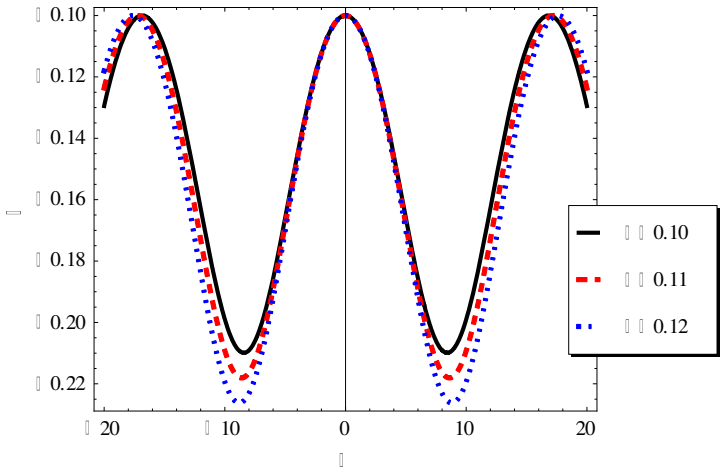

Fig.11. (Colour online) The evolution of the DAPTW,ϕ, for different values of β at $L_z = 0.18, \delta = 1.5, \sigma = 0.1, \alpha = 0.1$ and $\omega_c = 0.3$.

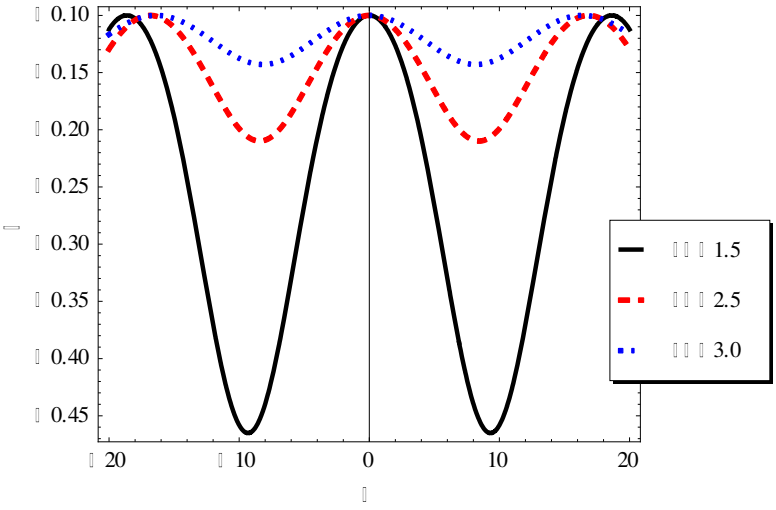

Fig.12. (Colour online) The evolution of the DAPTW,ϕ, for different values of α at $L_z = 0.18, \delta = 1.5, \beta = -2.5, \sigma = 0.1$ and $\omega_c = 0.3$.

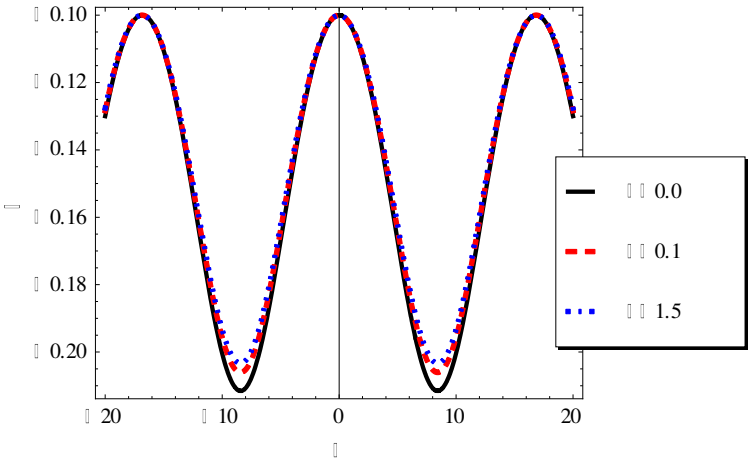

Fig.13. (Colour online) The evolution of the DAPTW,ϕ, for different values of ω_c at $L_z = 0.18, \delta = 1.5, \beta = -2.5, \sigma = 0.1$ and $\alpha = 0.1$.

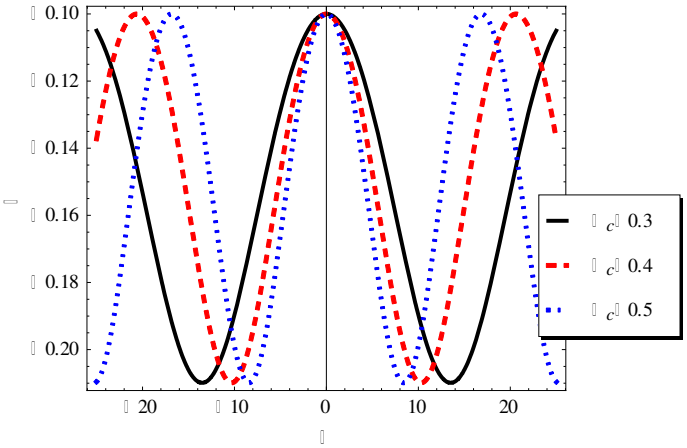

Data availability statement

The data that supports the findings of this study are available within the article.

References

Abdelwahed, H. G., El-Shewy, E. K., El-Depsy, A., El-Shamy, E. F.: Phys. Plasmas, **24**, 023703(2017)

Abdikian, A., Tamang, J., Saha, A.: Waves Complex Media, https://doi.org/10.1080/17455030.2021.1965242 (2021)

Adhikary, N. C., Deka, M. K., Dev, A. N. Sarma, J.: Phys. Plasmas,**21**, 083703(2014)

Adhikary, N.C., Misra, A.P., Deka, M.K. Dev, A.N.: Phys. Plasmas, **24**, 073703 (2017)

Cairns, R.A., Mamum, A.A., Bingham, R., Boström, R., Dendy, R.O., Nairn, C.M.C. and Shukla, P.K.: Geophys. Res. Lett., **22**,2709(1995)

Chow, S.N., Hale, J.K.: Method of Bifurcation Theory. Springer, New York (1981)

Dev, A.N., Sarma, J. Deka, M.K.:Can. J. Phys.**93**,1030 (2015)

Dev, A.N., Sarma, J., Deka, M.K. Adhikary, N.C.: Plasma Sci. Technol.**17**, 268 (2015)

El-Hanbaly, A.M., El-Shewy, E.K., Sallah, M. and Darweesh, H.F.:J. Theor. Appl. Phys. **9**,167(2015)

El-Shamy, E. F., Selim M. M., El-Depsy A., Mahmoud, M. Al-Hagan, O. Al-Mogeeth A.: Z. Naturforsch A. **75**, 921 (2020)

Fortov, V.E., Ivlev, A.V., Khrapak, S.A., Khrapak, A.G. and Morfill, G.E.: Complex (dusty) plasmas: Current status, open issues, perspectives. Phys. Rep. **421**,1 (2005)

Futaana, Y., Machida, S., Saito, Y., Matsuoka, A., Hayakawa, H.: J. Geophys. Res. **108**,1025 (2003)

Gill, T. S., Kaur, H., Bansal, S., Saini, N. S., Bala, P.: Eur. Phys. J. D **41** 151(2007)

Lundin, R., Zakharov, A., Pellinen, R., Borg, H., Hultqvist, B., Pissarenko, N., Dubinin, E. M., Barabash, S.W., Liede, I., Koskinen, H.: Nature, **341**,609(1989)

Mamun, A. A. Shukla, P. K.: Phys. Rev. E. **80**, 037401(2009)

Mamun, A. A.:PhysicaScripta, **57**, 258 (1998)

Mamun, A.A., Cairns, R.A. Shukla, P.K.: Phys. Plasmas, **3**,702(1996)Schamel, H.: Plasma Phys.**14**,905(1972)

Misra, A. P., Wang, Y.: Commun. Nonlinear Sci. Numer. Simulat. **22**, 1360 (2015)

Pradhan, P., Abdikian, A., Saha, A.: Eur. Phys. J. D **75**, 48(2021)

Saha, T. Chatterjee, P.: Phys. Plasmas, **16**, 013707 (2009)

Samanta, U. K., Saha, A., Chatterjee, P.: Phys. Plasmas, **20**, 052111(2013)

Schamel, H.:J. Plasma Phys. **9**, 377 (1973)

Schamel, H.: Phys. Rep. **140**,161(1986)

Selim, M. M., Abdelaleem, H., El-Bedwehy, N. A., El-Shamy, E. F.: Contrib. PlasmaPhys. doi. org/10. 1002/ctpp.202100153(2021)

Selim, M. M., El-Shamy, E. F., El-Depsy, A.: Astrophys. Space Sci. **360**, 66 (2015)

Selim, M. M.: Eur. Phys. J. Plus. **131**, 93 (2016)

Shukla, P. K., Mamun, A. A.: Introduction to Dusty Plasma Physics, Institute of Physics, Bristol (2002)

Sultana, S.: Chin. J. Phys. **69**,206 (2021)

Tolba, R. E.: Eur. Phys. J. Plus. **36**, 138(2021)

Washimi H., Taniuti, T.: Phys. Rev. Lett.**17**, 996(1966)